

Mass distributions for monoenergetic-neutron-induced fission of ^{235}U

L. E. Glendenin, J. E. Gindler, D. J. Henderson, and J. W. Meadows

Argonne National Laboratory, Argonne, Illinois 60439

(Received 7 August 1981)

Fission product yields for 37 masses were determined for the fission of ^{235}U with essentially monoenergetic neutrons of 0.17, 0.55, 1.0, 2.0, 4.0, 5.5, 6.3, 7.1, and 8.1 MeV. Fission product activities were measured by Ge(Li) γ -ray spectrometry of irradiated ^{235}U targets and by chemical separation of the fission product elements followed by β counting and/or γ -ray spectrometry. The mass-yield data show a sensitive increase of fission yields in the near symmetric mass region (valley) with increasing incident neutron energy E_n (peak-to-valley ratio decreasing from 590 to 13) over the range of 0.17 to 8.1 MeV with only small changes in yields in other regions of the mass distribution. Curves of valley yields as a function of E_n display a flat step in the region of second-chance fission (above ~ 6 MeV) where the excitation energy is lowered by competition with neutron evaporation prior to fission. Comparison is made with monoenergetic-neutron-induced fission of ^{238}U .

[NUCLEAR REACTIONS, FISSION $^{235}\text{U}(n,f)$, $E_n=0.17, 0.55, 1.0,$
2.0, 4.0, 5.5, 6.3, 7.1, and 8.1 MeV; measured mass yields.]

I. INTRODUCTION

Although essentially complete fission product mass distributions have been compiled^{1,2} for fission of ^{235}U by thermal, fission spectrum ("fast"), and 14-MeV ("high energy") neutrons, relatively little data are available on the characteristics of mass distributions for monoenergetic-neutron-induced fission (n_E, f), particularly as a function of incident neutron energy E_n . Ford and Leachman³ determined the yields of five fission products in the near-symmetric mass region ($A=109$ to 115) at eight E_n values in the range of 4.7 to 18 MeV. Ford and Norris⁴ have reported yields of a few fission products at neutron energies of 5 and 8 MeV. Cuninghame *et al.*⁵ measured the yields of five fission products at six neutron energies between 0.13 and 1.7 MeV. The yields of 28 mass chains were measured by Chapman *et al.*⁶ for four neutron energies in the range of 6.0 to 9.1 MeV, where second-chance fission becomes important.

The present work was undertaken to explore the characteristics of the mass distribution for $^{235}\text{U}(n_E, f)$ as a function of E_n over the range of 0.17 to 8.1 MeV. For this purpose, reasonably complete mass distributions (37 masses) were obtained at E_n values of 0.17, 0.55, 1.0, 2.0, 4.0, 5.0, 6.3, 7.1, and 8.1 MeV.

II. EXPERIMENTAL

A. Neutron irradiations

Targets for the neutron irradiations were 2.54-cm diameter by 0.0127-cm thick disks of uranium metal with an average weight of 1 g and an isotopic composition of 1.03% ^{234}U , 93.17% ^{235}U , 0.26% ^{236}U , and 5.54% ^{238}U . Irradiations were made at the Argonne Fast Neutron Generator Facility⁷ in the manner described by Smith and Meadows.⁸ The targets were attached to a low-mass fission chamber containing a thin, standardized deposit of ^{235}U to monitor the fission rate. This assembly was positioned about 3 cm from the neutron source. Neutrons with energies below 5 MeV were produced by the $^7\text{Li}(p,n)^7\text{Be}$ reaction and neutrons of higher energy by the $^2\text{H}(d,n)^3\text{He}$ reaction.

Details of the monoenergetic neutron beam characteristics have been given in a previous publication.⁹ Spread in the principal neutron energy was 2–3% for $E_n > 2$ MeV and 6–10% for $E_n < 2$ MeV. Fission rates in a target disk were typically $3 \times 10^4 \text{ sec}^{-1}$. Also present were small contributions to the fission rate by secondary neutrons of other energies arising from the $^7\text{Li}(p,n)^7\text{Be}^*$ reaction, from deuteron stripping

reactions (primarily in the deuterium target cell), and from elastic and inelastic scattering by the room environment. Small corrections (1–10%) were made for the effects of the secondary neutrons on the fission yields of masses that are strongly sensitive to neutron energy ($A=105$ to 129). Corrections were also made for the small contribution by $^{238}\text{U}(n_E, f)$ using yield data from Ref. 9. To ensure adequate intensities of fission product activities the targets were irradiated for periods of about 16 h.

B. Fission yield determinations

Fission yields were determined by high-resolution γ -ray spectrometry of an irradiated uranium target or by chemical separation of a fission product (or group of elements) followed by γ -ray spectrometry or β counting. These three methods are designated herein as the γ , RC- γ , and RC- β methods, respectively. Yields of rare earth fission products were determined by both the γ and RC- γ methods. For measurement of the low activities of fission products in the near symmetric (valley) mass region (109 to 127) it was necessary to employ the more sensitive RC- β method. The γ method was used for all other determinations.

For chemical separation of the fission product elements the irradiated uranium metal targets were dissolved in concentrated hydrochloric acid containing a little nitric acid and carriers for the elements of interest. Cerium was used as a group carrier for the rare earth elements. The elements were then separated, chemically purified, and samples prepared for β counting following the procedures compiled by Flynn.¹⁰ The samples were counted in a calibrated low-background (0.5 count/min) β proportional counter¹⁰ equipped with an automatic sample changer. The radioactive purity for each sample was verified by following its decay over an extended period of several half-lives. Decay curves were analyzed with the least-squares computer program CLSQ.¹¹ The observed β counting rate at the end of irradiation for each fission product was then corrected for chemical yield, counting efficiency, decay, genetic relationships, and degree of saturation during irradiation to give the saturation activity A_∞ .

For γ counting, the irradiated targets and rare earth samples were mounted on steel or aluminum plates and placed in a computer-controlled sample changer designed to ensure reproducible positioning of samples. The γ -ray spectrometer system was

based on an 80-cm³ lithium-drifted germanium Ge(Li) detector with a resolution of 2.2 keV (FWHM) for the 1.33-MeV γ -ray of ^{60}Co . Details of this system and the γ counting method are given in a previous publication.⁹ To enhance statistical accuracy in the determination of the fission product γ -ray activities a large number of γ -ray spectra (~ 40) were recorded over a sufficient period of time (~ 1 month) to encompass the wide range of half-lives involved. The spectra were then analyzed with the computer program GAMANAL¹² to obtain the intensities of the resolved photopeaks.

The measured fission product γ -ray activities were then analyzed by the decay program CLSQ¹¹ to obtain the activities at the end of irradiation. Further corrections were made as required for counting efficiency, cascade coincidence losses,⁹ absolute γ emission intensities,¹³ genetic relationships, and degree of saturation during irradiation to give the saturation activity A_∞ .

Values of A_∞ determined by the methods just described are related to fission yields by the expression

$$\text{fission yield} = A_\infty / \text{fission rate} .$$

In this work the fission rate was determined by two methods: (1) counting of a standard ^{235}U sample in a fission chamber; and (2) normalization of the mass distribution to 200% total yield, the undetermined yields being interpolated or extrapolated from measured yields. Since $\sim 60\%$ of the total yield was determined, the uncertainty (1σ) in the fission rate obtained by the normalization procedure is only 3% when a 20% error is assigned to all interpolated or extrapolated values. The normalization procedure to obtain the fission rate was used in all cases, with fission counting being employed in some of the irradiations. Agreement between the two methods was found to be within experimental error.

III. RESULTS AND DISCUSSION

The results of the fission product yield determinations are presented in Table I and shown graphically as mass-yield curves for several values of E_n in Fig. 1. Also shown for comparison in Fig. 1 are mass distributions for thermal and 14 MeV neutrons based on data from Ref. 1. Uncertainties (1σ) in the fission yield values were obtained by consideration of all known sources of random and systematic error with the usual rules

TABLE I. Fission product yields in monoenergetic-neutron-induced fission of ^{235}U . Standard errors in the yield values are given in parentheses as uncertainties in the last digits.

Fission product	Method	Incident neutron energy								
		0.17	0.55	1.0	2.0	4.0	5.5	6.3	7.1	8.1
^{84}Br	γ	1.70(26)		1.24(22)		1.40(21)				
$^{85}\text{Kr}^m$	γ	1.35(9)	1.74(13)	1.49(6)	1.76(11)	1.70(7)	1.81(10)	1.84(12)	2.37(14)	2.07(13)
^{87}Kr	γ	2.38(19)	2.48(15)	2.71(14)	2.81(16)	2.89(15)	2.86(16)	2.66(21)	3.05(20)	2.83(17)
^{88}Kr	γ	3.29(15)	3.26(19)	3.35(15)	3.22(17)	3.24(16)	3.22(16)	3.27(21)	3.43(19)	3.38(18)
^{89}Rb	γ	4.27(52)				4.22(56)	3.57(55)			
^{91}Sr	γ	5.82(23)	5.53(22)	5.81(23)	5.36(21)	5.20(20)	4.98(20)	4.87(19)	5.19(20)	5.15(21)
^{92}Sr	γ	5.78(42)	5.38(44)	5.86(67)	5.17(42)	5.22(36)	5.08(45)	4.73(39)	4.78(45)	4.79(39)
^{93}Y	γ	6.64(35)	6.36(55)	6.43(32)	6.62(40)	6.18(37)	5.88(50)	6.47(44)	6.20(44)	6.23(36)
^{94}Y	γ					5.87(42)	5.59(47)			
^{95}Zr	γ	6.81(36)	6.71(28)	6.57(25)	6.65(57)	6.39(28)	6.41(25)	6.27(33)	6.05(30)	6.14(32)
^{97}Zr	γ	5.91(22)	5.78(22)	6.12(23)	5.76(22)	5.92(23)	5.86(24)	5.58(23)	5.57(22)	5.47(23)
^{99}Mo	γ	5.94(27)	5.42(29)	5.71(30)	5.41(29)	5.45(29)	5.52(31)	5.05(29)	5.21(28)	4.92(27)
^{103}Ru	γ	3.60(19)	3.51(18)	3.44(18)	3.33(18)	3.57(19)	2.58(14)	3.52(19)	3.22(17)	3.08(17)
^{105}Ru	γ	1.11(8)	1.16(9)	1.23(6)	1.10(9)	1.42(9)	1.66(10)	1.60(17)	1.63(9)	1.53(9)
^{109}Pd	RC- β	0.027(5)	0.027(5)	0.047(7)	0.061(9)	0.16(2)	0.41(6)	0.39(6)	0.39(6)	0.54(8)
^{111}Ag	RC- β	0.016(2)	0.024(4)	0.023(3)	0.047(7)	0.14(2)	0.30(5)	0.30(5)	0.31(5)	0.43(6)
^{112}Pd	RC- β	0.012(2)		0.025(4)	0.048(7)	0.12(2)	0.23(4)	0.29(4)	0.23(4)	0.44(6)
$^{115}\text{Cd}^g$	RC- β	0.010(2)	0.017(3)	0.020(3)	0.051(8)	0.10(2)	0.28(4)	0.32(5)	0.34(5)	0.38(6)
$^{121}\text{Sn}^g$	RC- β	0.009(2)	0.014(2)	0.014(2)	0.033(5)	0.082(12)	0.21(3)	0.23(3)	0.23(3)	0.30(5)
$^{125}\text{Sn}^g$	RC- β	0.009(2)	0.015(2)	0.014(2)	0.033(5)	0.088(13)	0.18(3)	0.21(3)	0.20(3)	0.30(5)
^{127}Sb	RC- β	0.13(2)	0.14(2)	0.12(2)	0.23(3)	0.39(6)	0.78(12)	0.73(11)	0.78(12)	0.98(15)
^{129}Sb	γ , RC- β	0.89(7)	0.88(8)	0.99(13)	1.06(10)	1.41(15)	1.97(14)	1.72(15)	1.74(14)	1.75(14)
^{131}I	γ	3.53(18)	3.63(16)	3.56(14)	3.69(16)	4.00(17)	4.75(20)	4.98(21)	4.41(32)	4.36(18)
^{132}Te	γ	4.65(20)	4.69(21)	4.84(18)	4.73(19)	5.10(25)	5.17(20)	4.86(21)	4.85(19)	4.75(20)
^{133}I	γ	6.63(28)	6.69(29)	6.92(30)	6.37(27)	6.47(28)	6.34(27)	6.11(26)	6.22(27)	5.95(26)
^{134}Te	γ	6.18(30)	5.94(47)	6.46(32)	5.71(30)	4.71(24)	3.80(27)	3.60(44)	3.91(58)	3.74(51)
$^{134}\text{I}^a$	γ	0.80(60)	1.79(130)		2.13(100)	1.95(44)	2.65(92)	2.97(243)	3.27(156)	2.69(118)
^{135}I	γ	6.48(25)	6.29(24)	6.39(26)	6.32(24)	6.42(24)	6.23(24)	5.66(25)	5.83(22)	5.68(36)
$^{135}\text{Xe}^a$	γ	0.50(20)	0.38(22)		0.38(20)	0.46(30)	0.89(18)	0.81(24)	0.39(33)	
^{138}Xe	γ	5.32(31)	5.86(37)	5.87(32)	6.46(36)	6.10(57)	5.41(75)			5.23(30)
^{139}Ba	γ	6.27(46)	6.40(31)	6.91(47)	5.87(35)	6.42(37)	5.53(54)	5.57(43)		6.01(39)
^{140}Ba	γ	6.45(34)	6.30(25)	6.23(28)	6.11(24)	5.82(24)	5.66(24)	5.60(23)	5.51(22)	5.30(20)
^{141}Ce	RC- γ		6.37(57)		6.26(53)	6.03(79)	6.45(84)	5.70(49)	5.87(55)	5.57(43)
^{142}La	γ , RC- γ	5.35(36)	5.55(37)	5.61(39)	5.56(32)	5.16(36)	4.63(29)	4.85(33)	4.90(29)	4.68(27)
^{143}Ce	γ , RC- γ	5.57(26)	6.14(36)	5.50(36)	5.76(33)	4.66(43)	4.83(28)	4.90(30)	5.02(29)	4.92(28)
^{144}Ce	γ , RC- γ	5.26(59)			5.48(71)	4.19(44)			4.30(51)	4.65(55)
^{147}Nd	γ , RC- γ	2.18(18)	2.51(17)	2.33(22)	2.47(16)	2.22(10)	2.61(19)	2.27(17)	2.13(14)	2.22(15)
^{149}Pm	γ , RC- γ	1.17(11)	1.40(16)	1.24(15)	1.41(15)	1.15(10)	1.31(22)	1.49(19)	1.10(14)	1.12(12)
^{151}Pm	γ , RC- γ	0.43(3)	0.38(4)	0.40(4)	0.43(4)	0.52(3)	0.64(4)	0.58(5)	0.53(5)	0.53(3)

^aIndependent yield.

of error propagation. For peak fission yields (> 1%) measured by the γ and RC- γ methods uncertainties fall typically in the range of 4–10%. Larger uncertainties of about 15% are associated with the valley yields measured by the RC- β method. An assessment of possible error in determination of the mass yield due to direct formation in fission (independent yield) of chain members

beyond the one measured was made from the energy-dependent charge distribution systematics of Nethaway.¹⁴ The calculations show that the measured fission product yields over the E_n range of 0 to 8 MeV represent essentially total chain yields except for the independent yields of ^{134}I and ^{135}Xe . From the fission yields of the isomers $^{115}\text{Cd}^g$, $^{121}\text{Sn}^g$, and $^{125}\text{Sn}^g$ total chain yields may be es-

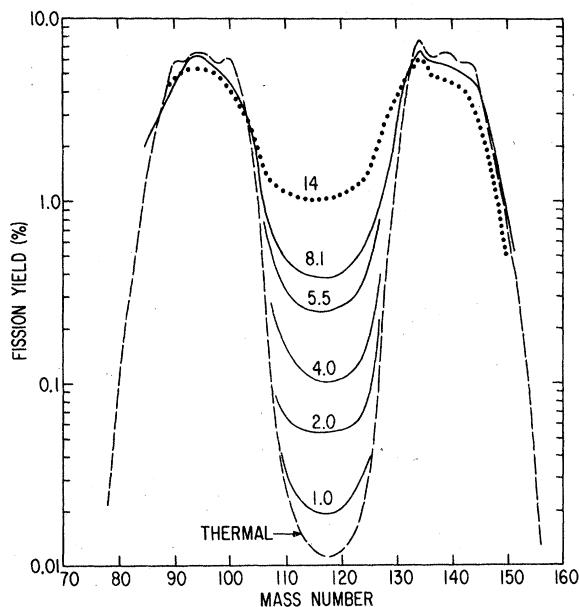


FIG. 1. $^{235}\text{U}(n_E, f)$ mass distributions. The solid curves represent the results of present measurements. The 14-MeV (dotted curve) and the thermal-neutron (dashed curve) data are taken from Ref. 1.

timated by using isomer ratios $(m+g)/g$ of 1.11 ± 0.05 for $^{115}\text{Cd}^g$ (average value for several fissioning systems in Ref. 1), 1.16 ± 0.11 for $^{121}\text{Sn}^g$,¹⁵ and about 2.4 for $^{125}\text{Sn}^g$.¹

The salient features apparent from the mass distributions shown in Fig. 1 are the strong dependence of fission yields in the valley mass region on E_n (increased probability of near-symmetric fission with increasing excitation energy) and the weak dependence of peak yields on E_n . These effects are illustrated in Fig. 2, where the yields of the valley fission products and a typical peak fission product (^{140}Ba) are plotted as a function of E_n . Also shown (at the bottom of the figure) is the cross section σ_F for neutron-induced fission of ^{235}U as a function of E_n with positions indicated by arrows at approximately 6 and 13 MeV, where second-chance fission (n, nf) and third-chance fission ($n, 2nf$) become energetically possible (causing steps in the σ_F curve). The data show clearly the effects of excitation energy on near-symmetric fission yields, i.e., the sensitive increase in yield with increasing neutron energy, and distinct steps in the curves following the onset of second-chance fission (near $E_n = 6$ MeV), for which excitation energy is lowered by competition with neutron emission prior to fission. In our previous work^{9,13} only a break in the slope of the yield vs E_n curve at 6

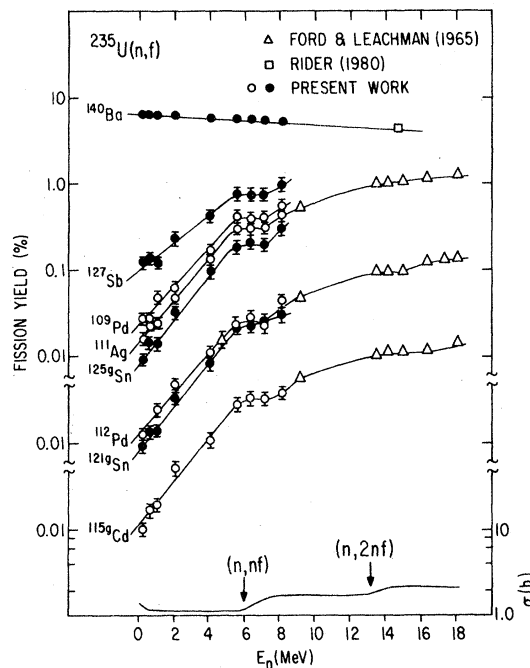


FIG. 2. Fission yields and cross section σ_F for fission of ^{235}U by monoenergetic neutrons as a function of neutron energy.

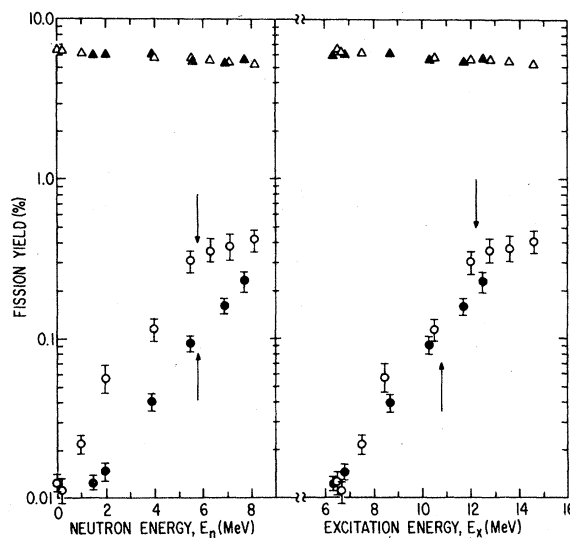


FIG. 3. The yields of ^{140}Ba (triangles) and ^{115}Cd (circles) for neutron-induced fission of ^{235}U (open symbols) and ^{238}U (closed symbols) as a function of (a) incident neutron energy and (b) excitation energy. Downward and upward pointing arrows indicate the energies at which the respective reactions, $^{235}\text{U}(n, nf)$ and $^{238}\text{U}(n, nf)$, become possible.

TABLE II. $^{235}\text{U}(n_E, f)$ mass distribution characteristics.

E_n	Peak-to-valley ratio ^a	Mean mass (μ)		$\bar{\nu}$ ^b	$\bar{\nu}$ ^c
		Light group	Heavy group		
0.17	590	94.9	138.6	2.5	2.44
0.55	330	94.9	138.7	2.4	2.48
1.0	290	94.9	138.5	2.6	2.53
2.0	110	94.9	138.6	2.5	2.64
4.0	51	95.2	138.0	2.8	2.92
5.5	19	95.4	137.7	2.9	3.18
6.3	16	95.5	137.6	2.9	3.28
7.1	15	95.2	137.6	3.2	3.48
8.1	13	95.4	137.5	3.1	3.62

^aPeak-to-valley ratio based on the yields of ^{140}Ba and ^{115}Cd ($m + g$).

^bCalculated from conservation of mass.

^cEvaluated from experimental measurements by fission-coincident neutron counting (Ref. 16).

MeV was seen for $^{238}\text{U}(n_E, f)$, whereas distinct dips in the curves were observed for $^{232}\text{Th}(n_E, f)$.

In contrast with the energy-sensitive valley region the yields of asymmetric fission products near the peaks of the mass distribution are only weakly dependent of E_n . This is illustrated by the data for ^{140}Ba plotted at the top of Fig. 2. The fission yield is seen to decrease monotonically by only $\sim 20\%$ over the E_n range to 0 to 14 MeV, as required to compensate for the increasing yields of the valley mass region.

A comparison of fission yield dependence on E_n for $^{235}\text{U}(n_E, f)$ (open symbols) and $^{238}\text{U}(n_E, f)$ (closed symbols) is shown in Fig. 3, where the yields of ^{115}Cd , a valley fission product, and ^{140}Ba , a peak fission product, are plotted as a function of E_n in Fig. 3(a), and in Fig. 3(b) as a function of excitation energy E_X , where $E_X = E_n + B_n$, and B_n is the binding energy of the captured neutron in the compound nucleus (6.47 MeV for ^{236}U and 4.78 MeV for ^{239}U). It is seen that as a function of ex-

citation energy the yields for the two fissioning systems are nearly the same, at least in the region where only first-chance fission can occur.

Some mass distribution characteristics derived from the fission yield data for monoenergetic-neutron-induced fission of ^{235}U are given in Table II. The relative change in mean mass for the light and heavy groups as a function of E_n indicates that the increase in neutron emission with increasing excitation energy is greater from the heavy fragment. Values of $\bar{\nu}$, the average number of neutrons emitted per fission, calculated from the mean masses are in reasonable agreement with experimental values based on direct measurement by fission-coincident neutron counting¹⁶ at $E_n < 5$ MeV but are somewhat low at higher values of E_n .

This work was supported by the U.S. Department of Energy, Division of Nuclear Physics, under Contract W-31-109-Eng-38.

¹B. F. Rider, Vallecitos Nuclear Center Report No. NEDO-12154-3(B), 1980.

²E. A. C. Crouch, At. Data Nucl. Data Tables **19**, 419 (1977).

³G. P. Ford and R. B. Leachman, Phys. Rev. **37**, 826 (1965).

⁴G. P. Ford and A. E. Norris, Los Alamos Scientific Laboratory Report No. LA-6129, 1976.

⁵J. G. Cuninghame, J. A. B. Goodall, and H. H. Willis, J. Inorg. Nucl. Chem. **36**, 1453 (1974).

⁶T. C. Chapman, G. A. Anzelon, G. C. Spitale, and D. R. Nethaway, Phys. Rev. C **17**, 1089 (1978).

⁷S. A. Cox and P. R. Hanley, IEEE Trans. Nucl. Sci. **12**, 108 (1971).

⁸D. L. Smith and J. W. Meadows, Nucl. Sci. Eng. **58**, 314 (1975).

⁹S. Nagy, K. F. Flynn, J. E. Gindler, J. W. Meadows, and L. E. Glendenin, Phys. Rev. C **17**, 163 (1978).

¹⁰K. F. Flynn, Argonne National Laboratory Report No. ANL-75-24, 1975.

- ¹¹J. B. Cummins, National Academy of Science—
National Research Council Publication No. NAS-NS-
3107, 1962, p. 25.
- ¹²R. Gunnink and J. B. Niday, Lawrence Livermore La-
boratory Report No. UCRL-51061, 1972.
- ¹³L. E. Glendenin, J. E. Gindler, I. Ahmad, D. J. Hen-
derson, and J. W. Meadows, Phys. Rev. C 22, 152
(1980).
- ¹⁴D. R. Nethaway, Lawrence Livermore Laboratory Re-
port Nos. UCRL-51538 and UCRL-51640, 1974.
- ¹⁵B. R. Erdal, J. C. Williams, and A. C. Wahl, J. Inorg.
Nucl. Chem. 31, 2993 (1969).
- ¹⁶F. Manero and V. A. Konshin, At. Energy Rev. 10,
637 (1972).